

## Origin of the Different Reconstructions of Diamond, Si, and Ge(111) Surfaces

F. Bechstedt, A. A. Stekolnikov, J. Furthmüller, and P. Käckell

*Institut für Festkörpertheorie und Theoretische Optik, Friedrich-Schiller-Universität, 07743 Jena, Germany*

(Received 9 February 2001; published 15 June 2001)

*Ab initio* calculations of the  $2 \times 1$ ,  $c(2 \times 8)$ , and  $7 \times 7$  reconstructions of the diamond, Si, and Ge(111) surfaces are reported. The  $\pi$ -bonded chain, adatom, and dimer-adatom-stacking fault models are studied to understand the driving forces for a certain reconstruction. The resulting energetics, geometries, and band structures are compared for the elemental semiconductors with different atomic sizes, and chemical trends are derived. We show why the lowest-energy reconstructions are different for the group-IV materials considered.

DOI: 10.1103/PhysRevLett.87.016103

PACS numbers: 68.35.Bs, 68.35.Md, 73.20.At

The origin and nature of reconstructions at (111) surfaces of elemental semiconductors is one of the most intensively discussed issues in surface physics. The (111) surfaces of diamond, silicon, and germanium show a manifold and puzzling reconstruction behavior in dependence on the surface preparation and the considered semiconductor. Silicon and germanium exhibit a  $2 \times 1$  reconstruction following cleavage perpendicular to the [111] direction at room temperature. However, such a  $2 \times 1$  reconstruction can also be found on the C(111) surface after careful preparation [1]. From many experimental and theoretical studies the (111)-(2  $\times$  1) surfaces are believed to have a  $\pi$ -bonded chain geometry [2]. In the case of Si and Ge the  $\pi$ -bonded chains are tilted [3,4], whereas, apart from one exception [5], converged total-energy calculations do not indicate either a chain buckling or a chain dimerization for diamond(111) [6–8]. For Si and Ge the  $\pi$ -bonded chain reconstruction has two different isomers with the tilt angle of the uppermost chains in opposite directions [4,9,10]. The chain-left isomer has been indeed observed for Ge(111)-(2  $\times$  1) by means of scanning tunneling microscopy [11]. Heat treatment of cleaved Si(111) and Ge(111) surfaces at elevated temperatures cause the  $2 \times 1$  reconstruction to convert into a  $7 \times 7$  (Si, [12]) and a  $c(2 \times 8)$  (Ge, [13]) structure, respectively. Whereas the Si(111)-(7  $\times$  7) surface is now explained by a dimer-adatom-stacking-fault (DAS) model with corner holes [14–17], the Ge(111)- $c(2 \times 8)$  surface is represented by a simple adatom model [18,19]. Recently, it has been shown that a  $c(2 \times 8)$  reconstruction can also be observed on the quenched Si(111) surface [20,21].

There are various *ab initio* studies of the basic reconstruction models, the  $\pi$ -bonded chain model for  $2 \times 1$  [4–9], the DAS model for  $7 \times 7$  [16,17], and the adatom model for  $c(2 \times 8)$  [19,21]. However, there is no study by one and the same group and one and the same method of all reconstructions for even one semiconductor, not to speak about the three group-IV materials under consideration. Therefore, a comparison of the energetics and the driving forces of the reconstruction is hardly possible. Precise conclusions, why the lowest-energy reconstructions  $2 \times 1$ ,  $7 \times 7$ , and  $c(2 \times 8)$  of diamond, silicon, or ger-

manium are different, cannot be drawn. Obviously, despite the same valence-electron structure of the atoms and the same crystal structure of the corresponding solid, the different atomic sizes and bonding characteristics give rise to a stabilization of different surface reconstructions. An explanation based on first-principles calculations is, however, still missing. There are only model considerations comparing the energetics of  $7 \times 7$  and  $c(2 \times 8)$  reconstructions [22].

In this Letter, we analyze the various reconstructions of the (111) surfaces of diamond, silicon, and germanium using *ab initio* total-energy minimization and electronic-structure calculations. Clear physical and chemical trends are observed for a given reconstruction model. The results are used to scrutinize the differences in the reconstruction behavior. We explain why the lowest-energy configurations of diamond and Si or Ge are so different by direct comparison, e.g., of the adatom geometries and the analysis of the accompanying electronic structures.

Our calculations are performed within the density functional theory (DFT) and the local density approximation (LDA). Explicitly we use a plane-wave-pseudopotential code [23]. The electron-ion interaction is described by non-norm-conserving ultrasoft pseudopotentials [24]. They allow the fully quantum-mechanical treatment of several hundreds of atoms in the supercell, even in the case of first-row elements. As a consequence, the plane-wave expansions can be restricted by cutoff energies of 19.8 Ry (C), 9.6 Ry (Si), and 8.8 Ry (Ge). The electron-electron interaction is described by the Perdew-Zunger parametrization of the Ceperley-Alder functional. The  $\mathbf{k}$ -space integrals over the Brillouin zone (BZ) are approximated by sums over Monkhorst-Pack (MP) special points. For the diamond structure the  $6 \times 6 \times 6$  MP mesh gives rise to lattice constants  $a = 3.531, 5.398, 5.627$  Å and fundamental energy gaps  $E_g = 4.15, 0.46, 0.00$  eV for C, Si, or Ge in DFT-LDA quality. In order to compute the energy gain for surfaces with incomplete atomic layers we use the calculated bulk chemical potentials  $\mu = -10.147, -5.957, \text{ and } -5.195$  eV/atom for C, Si, or Ge.

The surfaces are modeled by repeated slabs. Each slab consists of eight atomic layers and a sufficient amount of

vacuum layers. Adatoms are added on top of the slabs. Their bottom layers are passivated by hydrogen atoms and kept frozen during the surface optimization. The topmost five layers of the slab are allowed to relax. Converged results are obtained for the  $4 \times 8 \times 1$  ( $2 \times 1$ ),  $4 \times 4 \times 1$  [ $c(2 \times 8)$ ], and  $2 \times 2 \times 1$  ( $7 \times 7$ ) grids of MP points in dependence on the reconstruction.

The results for the energy gain with respect to the unreaxed (111) surface are listed in Table I for the three basic reconstructions  $2 \times 1$  ( $\pi$ -bonded chain model),  $c(2 \times 8)$  (adatom model), and  $7 \times 7$  (DAS model) of the C, Si, and Ge(111) surfaces. Our results agree with the experimental findings [1]. The most stable structures among the considered ones are the  $2 \times 1$  chain reconstruction for diamond, the  $7 \times 7$  translational symmetry of the complicated dimer-adatom-stacking fault surface with corner holes for silicon, and the  $c(2 \times 8)$  adatom surface for germanium. In the Ge case, we observe more or less the same energy gain for  $c(2 \times 8)$  and  $7 \times 7$ . This may be a consequence of limitations in the numerical accuracy. However, an indication for a near energetic degeneracy is the fact that the Ge(111)-( $7 \times 7$ ) surface can be also prepared in the presence of compressive biaxial strain [25]. It is also not clear whether the favorization of  $c(2 \times 8)$  against  $2 \times 1$  in the Si case is real or a consequence of numerical inaccuracies due to the use of different  $\mathbf{k}$ -point samplings. In any case, a long-range  $c(2 \times 8)$  ordering has been observed on the quenched Si(111) surface [20].

The comparison of the reconstructed with the relaxed (111) surfaces shows that relaxation in the Si and Ge cases gives a negligible effect. Only at the diamond surface relaxation is important. It is accompanied by a tendency for formation of a graphitelike overlayer [7]. The energy gains in Table I for the  $2 \times 1$  reconstructions are in good agreement with the results of other *ab initio* calculations [3,4,8,16,19]. This also holds for the differences of 0.06 eV (0.04 eV) between  $7 \times 7$  and  $2 \times 1$  for Si [16] ( $c(2 \times 8)$  and  $2 \times 1$  for Ge [19]). However, whereas the  $\pi$ -bonded chains on C(111) are undimerized and unbuckled, a remarkable buckling occurs for the two other group-IV materials. The corresponding buckling parameter, e.g., the difference in the vertical positions of two atoms forming a dimer, can be counted to be positive or negative resulting in a chain-right or a chain-left isomer [4,10]. In the case of the chain-right (chain-left) isomer we calculate a buckling parameter of 0.54 ( $-0.62$ ) Å for

Si and 0.82 ( $-0.83$ ) Å for Ge. The chain-left isomer has to be favored by 8 meV on Ge(111)-( $2 \times 1$ ), whereas for Si we find both isomers closer in energy with a difference of 5 meV.

The long-range  $c(2 \times 8)$  and  $7 \times 7$  reconstructions realize further energy gains with respect to  $2 \times 1$  for Si and Ge, at least for the adatom, DAS, and  $\pi$ -bonded chain models under consideration. However, the behavior of diamond(111) is completely different. Reconstruction elements like adatoms and corner holes are unfavorable. The different adatom behavior on C, Si, and Ge(111) is in agreement with earlier findings [26,27]. The reduction of the number of dangling bonds by adatoms indeed lowers the band structure energy contribution to the total energy. However, in contrast to Si and Ge, the strain in the backbonds due to displacements of adatom-terminated first-layer atoms and the rest atom limits the effective energy gain remarkably. For diamond the resulting surface stress is larger because of the stronger covalent bonds. Its bulk modulus is about 5 (6) times larger than in the Si (Ge) case. The strains are not very different. The lengths of the bonds between adatoms and first-layer atoms are 0.88 (1.06), 0.86 (1.05), and 0.88 (1.07)  $d_{\text{bulk}}$  for C, Si, or Ge(111)- $c(2 \times 8)$  [(111)-( $7 \times 7$ )] in units of the bulk bond length. The variation of the bond lengths of the rest atoms to the underlying atomic layer is larger, at least for  $c(2 \times 8)$ . We observe values of 0.72 (0.98), 0.81 (1.02), and 0.83 (1.03)  $d_{\text{bulk}}$  on C, Si, or Ge(111)- $c(2 \times 8)$  ( $7 \times 7$ ). The corresponding vertical distances are 0.25 (0.24), 0.47 (0.46), and 0.50 (0.50)  $d_{\text{bulk}}$ . Averaged values are given because these distances are, e.g., larger on the faulted half of the Si(111)-( $7 \times 7$ ) cell. Another argument is related to the varying number of atoms in the surface unit cell. Assuming that the reservoir of the atoms can be identified with the bulk crystal, energy contributions of  $-\frac{1}{4}\mu[c(2 \times 8)]$  and  $-\frac{4}{49}\mu(7 \times 7)$  occur with respect to  $2 \times 1$ . They are by about a factor of 2 larger for diamond and favor fourfold-coordinated C atoms.

Further arguments may be derived from the DFT-LDA band structures presented in Fig. 1. In the  $2 \times 1$  case the bands are presented for the unbuckled chain reconstruction (C) and the chain-left isomer (Si, Ge). One observes a clear chemical trend of the positions of the  $\pi$ - and  $\pi^*$ -chain bands in the fundamental gap with respect to the bulk valence-band maximum (VBM) as well as of the surface-state gap at  $J$ . Along the row  $C \rightarrow \text{Si} \rightarrow \text{Ge}$  the gap is opened as a consequence of the chain buckling. The occupied  $\pi$  bands are shifted below the VBM indicating an energy gain due to the band structure contribution. Nevertheless, this gain does not cause an energetical favorization of Ge(111)-( $2 \times 1$ ) versus Ge(111)- $c(2 \times 8)$ .

The stabilization of Ge(111)- $c(2 \times 8)$  becomes much clearer from the band structures in the middle panels of Fig. 1. Essentially the dangling bonds belonging to the two adatoms and the two rest atoms appear in the fundamental

TABLE I. Calculated reconstruction-induced energy gain (in eV) per ( $1 \times 1$ ) surface unit cell for three group-IV semiconductors. Gains due to relaxation are given for comparison.

Reconstruction	C	Si	Ge
Relaxed	0.57	0.06	0.01
$2 \times 1$	1.37	0.30	0.23
$c(2 \times 8)$	0.39	0.33	0.27
$7 \times 7$	0.34	0.36	0.27

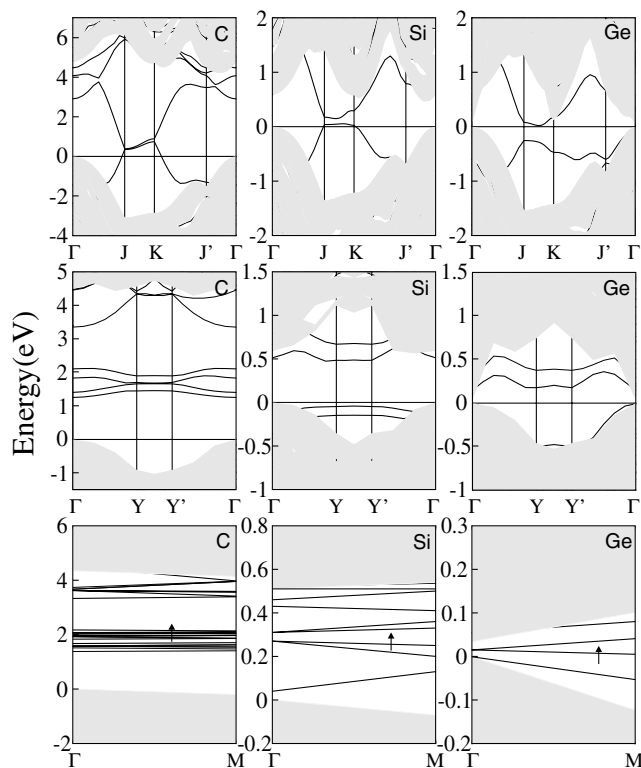


FIG. 1. Surface band structures versus high-symmetry directions in the corresponding two-dimensional Brillouin zone. The projected bulk band structures around the fundamental gap are presented as shaded areas. Upper panels:  $(2 \times 1)$   $\pi$ -bonded chain model; middle panels:  $c(2 \times 8)$  adatom model; and lower panels:  $(7 \times 7)$  DAS model. In the latter case the half-occupied band is indicated by an arrow.

gap region in the projected bulk band structure. The four bands are clearly observable for diamond because of the weak interaction of the dangling bonds and the similarities in the adatom and rest atom bonding to the underlying atomic layer. There is only a vanishing surface-state gap. In the silicon case the adatom dangling bonds become more  $p_z$ -like, whereas the rest atom dangling bonds increase the  $s$  character. As a consequence, the occupied surface bands belonging to the rest atoms are close to the VBM. In the Ge case, the occupied rest atom bands are shifted farther into the projected bulk valence bands. The accompanying energy gain via the band structure energy explains why the  $c(2 \times 8)$  reconstruction is energetically more favorable than the  $\pi$ -bonded chain  $2 \times 1$  reconstruction as well as why this happens in particular for germanium. The surface bands are clearly related to the geometry discussed above. Whereas the adatom structure is similar for C, Si, and Ge, there is an increase of the vertical distance of the rest atoms to the atomic layer beneath, 0.25, 0.47, and 0.50  $d_{\text{bulk}}$ . It is accompanied by a dehybridization from four  $sp^3$ - to  $p_x$ -,  $p_y$ -,  $p_z$ -, and  $s$  orbitals and, hence, a down-shift of the surface bands related to the occupied rest atom dangling bonds.

The lower panels in Fig. 1 give an idea about the stabilization of the  $7 \times 7$  DAS surface in the case of the larger group-IV atoms, in particular Si, with respect to the diamond case. The dangling bonds of the rest atoms, adatoms, and corner-hole atoms give rise to many bands in the fundamental gap of the bulk band structure projected onto the small BZ of the  $7 \times 7$  surface. The rest atoms dominate the occupied bands just below the Fermi level. It is pinned by the half-filled band at about 1.9, 0.3, and 0.02 eV, which is essentially formed by corner-hole states. According to their geometry, rest atoms behave similarly as discussed for  $c(2 \times 8)$ . Adatom dangling bonds give remarkable contributions to the unoccupied surface bands, e.g., near the conduction band minimum of diamond. However, center adatoms also contribute to bands close to  $E_F$ . The stronger localization of C dangling bonds results in less dispersive bands, whereas the stronger surface band dispersion tends to smear out the Si and Ge gaps. One observes a clear chemical trend along the row  $C \rightarrow Si \rightarrow Ge$  of shifting the occupied surface bands closer to the VBM or below and, hence, stabilizing the  $7 \times 7$  surface. This trend in particular follows our observation of the variation in the rest atom bonding.

In summary, we have presented *ab initio* studies for the basic reconstructions  $2 \times 1$ ,  $c(2 \times 8)$ , and  $7 \times 7$  of the (111) surfaces of the group-IV semiconductors diamond, silicon, and germanium. The resulting energetics has been discussed in terms of the most important structural parameters and surface band structures of the  $\pi$ -bonded chain, adatom, and dimer-adatom-stacking fault models. Chemical trends have been derived that indicate clear differences between the carbon atoms with a lack of  $p$  and  $d$  electrons in the core and the bigger Si or Ge atoms. Our first-principles results highlight the physical origin for the different reconstruction behavior. In particular, the strong C-C bonding is responsible for the lack of long-range adatom-induced reconstructions on diamond(111). Si and Ge surface structures gain more energy by the electron transfer between adatoms and rest atoms because of the accompanying smaller subsurface stresses. In the intermediate case of silicon, additional reconstruction elements occur to balance the different tendencies observed for diamond and germanium.

This work has been supported by the Deutsche Forschungsgemeinschaft (Sonderforschungsbereich 196, Project No. A8). We acknowledge grants of computer time from the John von Neumann Institute for Computing Jülich and the Höchstleistungsrechenzentrum Stuttgart.

- 
- [1] W. Mönch, *Semiconductor Surfaces and Interfaces* (Springer, Berlin, 1995).  
 [2] K.C. Pandey, Phys. Rev. Lett. **47**, 1913 (1981); **49**, 223 (1982).

- [3] J. E. Northrup and M. L. Cohen, *Phys. Rev. Lett.* **49**, 1349 (1982).
- [4] N. Takeuchi, A. Selloni, A. I. Shkrebtii, and E. Tosatti, *Phys. Rev. B* **44**, 13 611 (1991).
- [5] S. Iarlori, G. Galli, F. Gygi, M. Parrinello, and E. Tosatti, *Phys. Rev. Lett.* **69**, 2947 (1992).
- [6] B. N. Davidson and W. E. Pickett, *Phys. Rev. B* **49**, 11 253 (1994).
- [7] A. Scholze, W. G. Schmidt, and F. Bechstedt, *Phys. Rev. B* **53**, 13 725 (1996); W. G. Schmidt, A. Scholze, and F. Bechstedt, *Surf. Sci.* **351**, 183 (1996).
- [8] G. Kern, J. Hafner, and G. Kresse, *Surf. Sci.* **366**, 445 (1996); **366**, 464 (1996).
- [9] S.-H. Lee and M.-H. Kang, *Phys. Rev. B* **54**, 1482 (1996).
- [10] M. Rohlfing, M. Palumbo, G. Onida, and R. Del Sole, *Phys. Rev. Lett.* **85**, 5440 (2000).
- [11] H. Hirayama, N. Sugihara, and K. Takayanagi, *Phys. Rev. B* **62**, 6900 (2000).
- [12] R. E. Schlier and H. E. Farnsworth, *J. Chem. Phys.* **30**, 917 (1959).
- [13] P. W. Palmberg and W. T. Peria, *Surf. Sci.* **6**, 57 (1967).
- [14] K. Takayanagi, Y. Tanishiro, M. Takahashi, and S. Takahashi, *J. Vac. Sci. Technol. A* **3**, 1502 (1985); *Surf. Sci.* **164**, 367 (1985).
- [15] G.-X. Qian and D. J. Chadi, *Phys. Rev. B* **35**, 1288 (1987).
- [16] K. D. Brommer, M. Needels, B. E. Larson, and J. Joannopoulos, *Phys. Rev. Lett.* **68**, 1355 (1992).
- [17] I. Stich, M. C. Payne, R. D. King-Smith, J.-S. Lin, and L. J. Clarke, *Phys. Rev. Lett.* **68**, 1351 (1992).
- [18] R. S. Becker, B. S. Swartzentruber, J. S. Vickers, and T. Klitsner, *Phys. Rev. B* **39**, 1633 (1989).
- [19] N. Takeuchi, A. Selloni, and E. Tosatti, *Phys. Rev. Lett.* **69**, 648 (1992).
- [20] M. Koike, Y. Einaga, H. Hirayama, and K. Takayanagi, *Phys. Rev. B* **55**, 15 444 (1997).
- [21] N. Takeuchi, *Phys. Rev. B* **57**, 6255 (1998).
- [22] D. Vanderbilt, *Phys. Rev. B* **36**, 6209 (1987).
- [23] G. Kresse and J. Furthmüller, *Comput. Mater. Sci.* **6**, 15 (1996); *Phys. Rev. B* **54**, 11 169 (1996).
- [24] J. Furthmüller, P. Käckell, F. Bechstedt, and G. Kresse, *Phys. Rev. B* **61**, 4576 (2000).
- [25] H. J. Gossmann, J. C. Bean, L. C. Feldman, E. G. McRae, and I. K. Robinson, *Phys. Rev. Lett.* **55**, 1106 (1985).
- [26] R. D. Meade and D. Vanderbilt, *Phys. Rev. B* **40**, 3905 (1989).
- [27] F. Bechstedt, W. G. Schmidt, and A. Scholze, *Europhys. Lett.* **35**, 585 (1996).